9th Asia-Pacific Conference on Wind Engineering
Auckland, New Zealand
3-7 December 2017

A numerical study of wind fields near ground induced by moving downbursts

Yumi Iida[1], Kiyotoshi Otsuka[1] and Yasushi Uematsu[2]

[1]Technical Research Institute of Obayashi Corporation,
4-640, Shimokiyoto, Kiyose, Tokyo, Japan

[2]Department of Architecture and Building Science,
Tohoku University, 6-6-11, Aoba, Aramaki, Aoba-ku, Sendai, Japan

Abstract

Wind fields near the ground surface induced by downbursts were investigated by conducting a series of numerical simulations using the large eddy simulation (LES) technique, where cases of traveling downbursts are included. The simulation model was verified with the experimental results obtained from a downburst simulator. The experiment focused on the horizontal profile of the maximum gust winds, as well as their areas and magnitudes. The results showed that the traveling downbursts reduced the maximum gust wind speeds.

Introduction

Severe winds such as tornadoes and downbursts can produce wind gusts strong enough to seriously damage buildings and, occasionally, injure people. The damage produced by these winds is due not only to the strengths of the winds, but also the wind borne debris the winds blow up from the ground. Therefore, it is important to understand the aerodynamic nature of severe winds near the ground. Meteorological studies on the mechanisms and predictions of severe winds have focused on the structures of the phenomena as a whole, including parent clouds, than on the fine structures of severe winds close to the surface, which might become important in engineering aerodynamics. Only a few studies have investigated the characteristics of severe winds near the ground, for example, from 0 to 100 m above the ground, where buildings and structures usually exist. Moreover, few studies have been conducted on downburst-produced wind fields. Therefore, the purpose of this study was to investigate characteristics of downburst flows near the ground.

A downburst is defined as an intense downdraft impacting the ground and then spreading horizontally as a strong wind gust. The downburst's rapid change in wind direction at lower heights where peak velocities occur is one of the most remarkable features that distinguishes it from the usual boundary layer flows and other wind hazards, except whirl winds. In addition, the movement of the downdraft with the parent cloud is another notable feature that makes the flow field more complicated.

In many of the previous engineering studies on downbursts, downbursts were generated by impinging jets both in the experiments and numerical simulations. Chay and Letchford [1], Mason et al. [2] and Letchford and Chay [3] conducted experiments using impinging jets, where three types of jets, that is, stationary jets, pulsed jets, and moving jets, were examined. Chay and Letchford [1] discussed the characteristics of the mean wind profiles using a stationary jet that kept blowing at a constant intensity for the entire duration of the experiments. Mason et al. [2] and Letchford and Chay [3] investigated the characteristics of the unsteady pulsed jet and the moving jet.

The authors also conducted experiments using the stationary jet and the pulsed jet using the facilities [4]. However, it was difficult to measure wind speeds over a broad area simultaneously in the experiments. In order to overcome the difficulties inherent in physical experiments, we decided to run numerical simulations using the large eddy simulation (LES) technique. The conditions of the numerical simulations were determined so that the model could reproduce the flows of the pulsed jet generated by the device in the experiments. Therefore, the velocity data could be readily obtained, even for points where data acquisition was difficult in the experiments.

Movement of the downburst with the parent clouds, which is one of the common features of downbursts, was also investigated. The influences of the moving speed on the peak velocities are discussed in this paper using three different moving speeds.

Numerical model and Methodology

Large eddy simulations (LES) were conducted using OpenFoam 2.1.0. Two types of downburst jet models were considered: the pulsed jet model and the moving jet model. The former models a jet that hits the ground and spreads out into all horizontal directions, while the latter models a jet that moves along a given line at a constant speed. It should be noted that, although the negative buoyancy is the primary driving force of downbursts in the real world, the jet treated here did not include the effects of buoyancy forces.

In the followings sections of this paper, the wind speed V_{jet}, which is defined as the velocity of the down flow at the center of a downburst at the height of 1 diameter of the downburst, is used as the velocity scale for normalization of velocities. The values of V_{jet} are set to 8.67 m/s and 3.45 m/s for the pulsed and moving jet models, respectively. Furthermore, the spatial distances are normalized by the diameter of the jet, i.e., D = 0.6 m.

Pulsed jet model

The dimensions and the computational conditions for the pulsed jet model are shown in figure 1 and table 1, respectively. This condition was determined based on our previous experiment [4]. The governing equations may be given as follows.

$$\frac{\partial u_i}{\partial x_i} = 0 \tag{1}$$

$$\frac{\partial u_i}{\partial t} + \frac{\partial u_j u_i}{\partial x_j} = -\frac{1}{\rho}\frac{\partial p}{\partial x_i} + \frac{\partial}{\partial x_j}\left(\nu \frac{1}{2}\left(\frac{\partial u_i}{\partial x_j} + \frac{\partial u_j}{\partial x_i}\right)\right) \tag{2}$$

where u_i and x_i represent the i-th component of velocity (m/s) and the coordinate in space (m), respectively; t is time (s); ρ is air density (kg/m^3); p is pressure (N/m^2); and ν is the SGS eddy viscosity coefficient (m^2/s).

The input data used for the inflow condition on the inlet surface shown in figure 1 was generated by using the experimental data expressed as the time history of velocity distribution on this

surface. The experimental data were obtained every 0.05 m from the center of the jet just below the inlet surface of the fan, as shown in figure 2(a). A linear interpolation was applied to the experimental data in order to obtain a smooth velocity distribution with a special resolution of 0.01 m. The velocity distribution was assumed to be axisymmetric, and the interpolated data were provided at a step of one degree in the circumferential direction θ (see fig. 2(b)).

Moving jet model

The dimensions of the moving jet model are shown in figure 3. The computational conditions were almost the same as those for the pulsed jet model mentioned above. The governing equations of this model are also given by equations (1) and (2). The driving force of the translational motion of the moving jet was expressed as an external force by adding a term given by equation (3) to the right hand side of equation (2) at the grid points included in the shaded cylindrical volume in figure 3.

$$F = -\eta(u^{t-1} - U^*) \qquad (3)$$

where u^{t-1} is the velocity at the previous time step (m/s); η is a kind of relaxation coefficient representing the inverse of the time scale (1/s), with which the velocities in the shaded cylindrical volume converge to U^*, where U^* is a prescribed constant velocity (m/s); U^* = 6.0 m/s.

A downburst generally moves with its parent clouds. According to the previous observations made in the middle latitude zone, the moving speed of the parent clouds ranged from 30 to 100 km/h, i.e., 10.8 to 26 m/s. Assuming that the maximum velocity U_{max} induced by the downburst was approximately 70 m/s, the V_{move}/U_{max} ratio roughly ranged from 0.1 to 0.4. Thus, three speed ratios of V_{move}/U_{max}, i.e., 0.1, 0.2 and 0.3, were chosen as representative values in the analysis.

Verification of the Numerical Model with the Experimental Results

Figure 4 shows the peak velocity profiles at four locations from the center of downburst (x/D = 0.33, 0.67, 1, and 1.33), at which the results for the pulsed jet model were compared with the experimental results. Considering a scatter in the experimental values, the maximum and minimum velocities among 10 runs were plotted in the figure. Although the simulated values were close to the minimum of the experimental results at x/D = 0.33, the results generally lay between the maximum and minimum values. Thus, we concluded that the computational model and conditions used in the present study were appropriate for the downburst simulations.

	Pulsed jet model	Moving jet model
The number of mesh	5,908,942	12,106,800
Numerical schemes	Time scheme: Euler Advective term: Linear with filtering for high-frequency ringing Viscous item (diffusion term): Second-order finite different method	
Ceiling/side Wall BC	p: 0, other: zero gradient	
Lower/ground BC	U, k: 0, other: zero gradient	
Algorithm	PISO (Pressure Implicit with Splitting of Operators)	
Turbulence model	NRCSM (Coherent structure smagorinsky model)	

Table 1: Analytic Conditions.

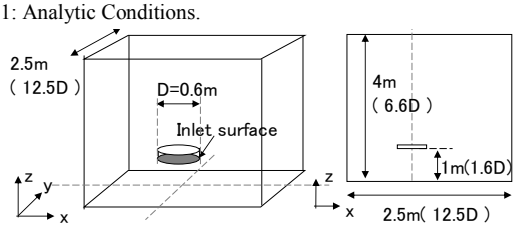

Figure 1. Analysis domain of the pulsed jet model.

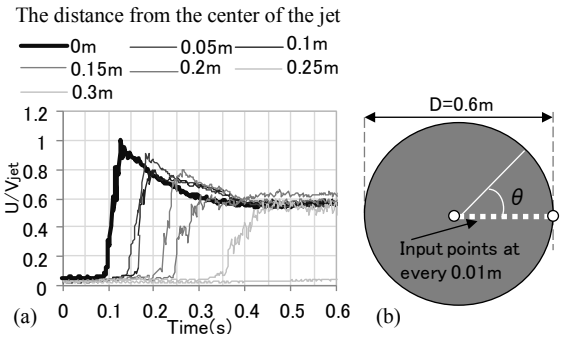

Figure 2. Inlet conditions of the pulsed jet model. (a) Time histories at each point from the centre of the jet in the experiment. (b) Inlet surface in figure 1.

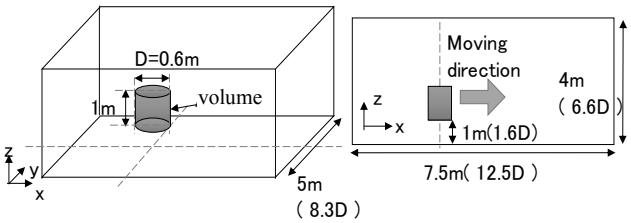

Figure 3. Same as Fig 1 but for the moving jet model.

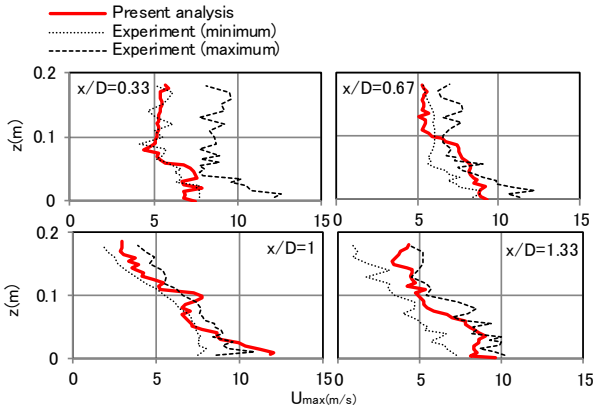

Figure 4. Comparisons between numerical simulation and experiment for pulsed jet.

Results and discussion

Scaling

In the present study, we assumed that λ_V = 1/2000, resulting in a time scale of $\lambda_T = \lambda_L/\lambda_V$ = 1/289 and 1/115 for the pulsed and moving jet models, respectively. The instantaneous maximum wind velocity U_{max} is obtained from the time history of wind velocity, to which a moving average of 3 s has been applied.

In the following sections, the characteristics of the wind velocities near the ground will be discussed based on the velocity at a height of z/D = 0.03, because El-Sayed Abd-Elaal [5] showed that the maximum instantaneous wind velocity generally occurred at heights of z/D ranging from 0.01 to 0.03.

Characteristics of the Maximum Velocity

In this section, the flow field of the pulsed jet model is compared with that of the moving jet model with a moving speed of V_{move}/V_{jet} = 0.2.

The variation in U_{max} at y/D = 0 (along the x axis) for the pulsed and moving jet models are shown in figure 5. In both cases, the jet starts to flow at x/D = 0. The downburst remains still at this

point in the pulsed jet case, while it moves in the x direction at a constant speed V_{move} in the moving jet case. The peak values appear at $x/D \approx \pm 1$ for the pulsed jet model, while the peak value occurs only at $x/D \approx 1$ for the moving jet model. The peak values at $x/D \approx 1$ for both models are almost the same. Differences between these two models also exist in the way the outflow winds propagate horizontally just after hitting the surface of the ground. The values of U_{max}/V_{jet} for $x/D > 2$ are almost the same, i.e., $U_{max}/V_{jet} = 0.8$–0.9, for the moving jet model. On the other hand, the value peaks at $x/D \approx 1$ and then decreases significantly with x/D for the pulsed jet model. These results indicate that the maximum peak velocity is primarily caused by the initial impact of the downflow to the ground in both cases.

Table 2 shows the maximum peak velocity and its location for each model. The U_{max}/V_{jet} value occurs at a location of x/D = 3.30 and y/D = 1.42, not on the traveling line of the moving jet (i.e., the x-axis) for the moving jet model. Furthermore, the value of U_{max}/V_{jet} is somewhat smaller than that for the pulsed jet model. This implies that the effect of movement of the jet on the maximum peak velocity near the ground is relatively small.

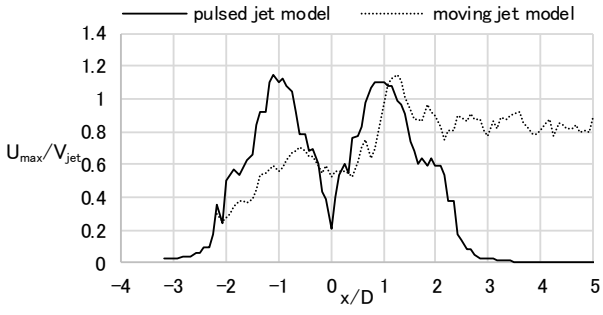

Figure 5. Horizontal velocity profiles of the maximum values of U_{max}/V_{jet} along the x-axis.

	x/D	y/D	U_{max}/V_{jet}
pulsed jet model	-1.00	0.08	1.28
moving jet model	3.30	-1.42	1.17

Table 2. Maximum peak velocity and its location.

To discuss the driving mechanism that produces the maximum peak velocity near the ground for both types of jets, the time history of normalized velocities at the two points shown in table 2 are studied. Figure 6 shows the results. A very sharp peak in wind velocity can be seen in both cases. However, the behavior after this peak is different between the two models. The time at which the second peak occurs is quite different for the two models. This feature implies that the secondary vortex, which subsequently occurs after the primary vortex [2] and generates the second peak velocity, is significantly influenced by the translational motion of the jet.

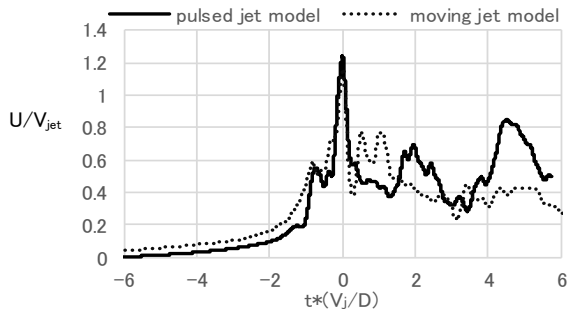

Figure 6. Time history of U_{max}/V_{jet} at the points where the maximum velocity occurred.

The spatial distributions of the maximum velocity for the pulsed and moving jet models are shown in figure 7. Downdraft starts at x/D = 0, y/D = 0, and the jet moves along the x axis. In both models, the effects of the initial hitting of the flow on the ground and the generation of the primary vortex can be recognized in an area given by $\sqrt{(x/D)^2 + (y/D)^2} < 1$.

In order to investigate the effect of translational motion of the jet on the maximum wind speeds U_{max}, the frequency distribution of U_{max} obtained at all grid points in an area defined by $0 < x/D < 2.5$ and $0 < y/D < 2.5$ is obtained. Figure 8 shows the results of the relative frequency for the pulsed and moving jet models, in which the class width of U_{max}/V_{jet} for obtaining the frequency is set to 0.1.

It is found that the relative frequency of larger values of U_{max}/V_{jet} is higher for the moving jet than for the pulsed jet. For example, the relative frequency of U_{max}/V_{jet} ranging from 0.75 to 0.85 is approximately 26% for the moving jet. This feature means that the moving jet expands the area of relatively higher wind speeds. Thus, it is thought that the moving jet increases the area swept by the downburst outflow winds. On the contrary, the moving jet somewhat decreases the relative frequency of U_{max}/V_{jet} larger than 1.0 and reduces the maximum wind velocity compared with the pulsed jet. It may be concluded that the moving jet breaks the primary vortex to some degree, resulting in a decrease in the maximum wind velocity.

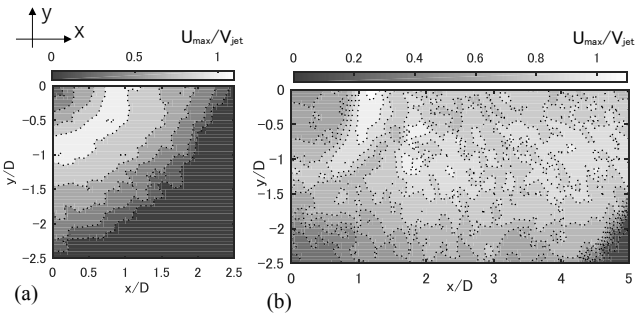

Figure 7. The distribution of the maximum velocity. (a) Pulsed jet model. (b) Moving jet model.

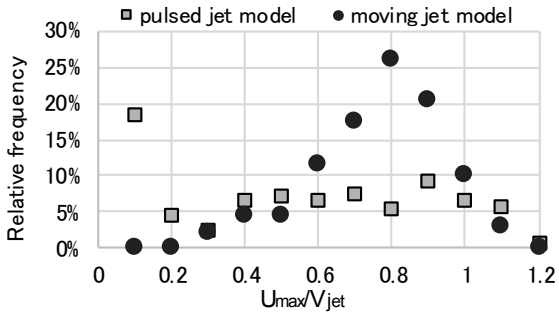

Figure 8. The frequency distribution in the area, $0 < x/D < 2.5$ and $0 < y/D < 2.5$.

Effect of Moving Speed

Figure 9 shows the horizontal profiles of U_{max}/V_{jet} at y/D = 0 for the moving jet model with three moving speeds, i.e., for V_{move}/V_{jet} of 0.1, 0.2 and 0.3. When the jet starts to flow (t = 0), the center of the jet is located at x/D = 0. The moving speed of the jet significantly affects the maximum peak velocities of the outflow winds. The highest velocity at $x/D \approx 1.0$, when V_{move}/V_{jet} = 0.1, is almost twice as large as that when V_{move}/V_{jet} = 0.3. Table 3 shows the maximum wind velocity and its location for each moving speed. While the initial peak caused by the primary vortex can be seen in all cases, the maximum values of U_{max}/V_{jet}

do not occur around $y/D = 0$, which suggests that the maximum velocity cannot be achieved easily on the moving line when the moving speed of the jet is relatively low, for example, when V_{move}/V_{jet} falls between 0.1–0.2. When $V_{move}/V_{jet} = 0.3$, the value of U_{max}/V_{jet} is fairly small. This means that higher moving speeds reduce the maximum peak velocity and may change the mechanisms producing the maximum velocity.

Moving jet model	x/D	y/D	U_{max}/V_{jet}
V_{move}/V_{jet} =0.1	2.42	-1.42	1.30
V_{move}/V_{jet} =0.2	-0.25	-1.42	1.17
V_{move}/V_{jet} =0.3	1.08	-0.08	0.81

Table 3. Maximum velocity and its location.

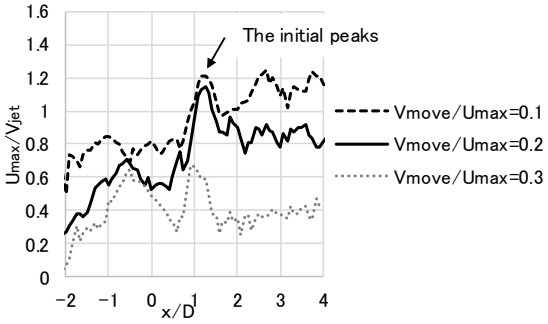

Figure 9. Horizontal profile of the maximum velocity along the x-axis.

Effects of Directions of the Moving Path on the Area of Strong Wind

Next, the influences on the maximum velocity of the relative location of the place under consideration (refer to 'recording point', hereafter) with respective to the center of the downburst at an instant when the downflow starts, which is represented by the distance r and the direction θ, as shown in figure 10. Figure 10 also shows the three areas denoted as A, B and C to be used in the following discussion.

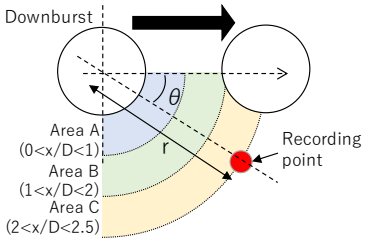

Figure 10. The definition of the direction θ of the path and the distance r of the recording point and the focused areas.

Figure 11 represents the relationships between U_{max}/V_{jet} at the recording point and the moving direction θ for the three areas. The moving speed of $V_{move}/V_{jet} = 0.2$ is chosen in this case. The results are shown for each of the three areas separately, because the tendencies of the results are significantly different from each other. It is seen that the values of U_{max}/V_{jet} in area A is almost independent of θ as well as of the moving direction of downburst relative to the recording point. On the other hand, the values of U_{max}/V_{jet} in areas B and C are significantly dependent on θ. The maximum velocities are generally larger than those in area A. The maximum velocity occurs in area B when $\theta = 0°$, which is somewhat larger than that observed in area C when $\theta = 30°$. It is also found that U_{max}/V_{jet} is reduced in magnitude by about 20 % of the maximum of U_{max}/V_{jet} irrespective of the distance r when $\theta > 45°$.

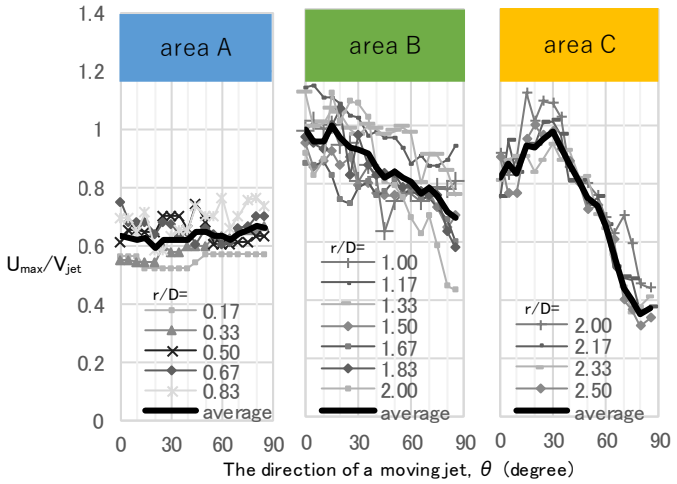

Figure 11. Relationships between the angles of the moving paths in the three areas of the flow field.

Conclusions

In the present study, a series of large eddy simulations of downbursts are conducted to understand the characteristics of the associated strong wind fields near the ground surface using two kinds of jet models: the pulsed jet model and the moving jet model. In addition, the influences of moving speed and moving direction on the peak velocities near the ground are discussed.

The area and the magnitude of the strongest downburst wind are significantly affected by the moving speed and the moving direction. These results will prove useful in finding the worst case that should be tested in a practical construction project, depending on the level required for the wind loading on structures, as well as for the influences of wind borne debris produced by the downburst. In the next stage of our study, we will simplify the numerical results and derive a semi-analytical formulation of the wind velocity distributions that can be used in downburst resistant design of buildings.

References

[1] Chay, M.T., Letchford, C.W., Pressure distributions on a cube in a simulated thunderstorm downburst, Part A: stationary downburst observations, *J. Wind Eng. Ind. Aerodyn.*, 90, 2002, 711–732.

[2] Mason, M., Letchford, C. W, and James, D., Pulsed wall jet simulation of a stationary thunderstorm downburst, part a: Physical structure and flow field characterization, *J. Wind Eng. Ind. Aerodyn.*, 93, 2005, 557–580.

[3] Letchford, C.W., Chay, M.T., Pressure distributions on a cube in a simulated thunderstorm downburst. Part B: moving downburst observations, *J. Wind Eng. Ind. Aerodyn.*, 90, 2002, 733–753.

[4] Iida, Y., Uematsu, Y., Gavanski, E., A study of downburst-induced wind loading on buildings. *J. Wind Eng.*, JAWE, 40(2), 2015, 40–49. (in Japan)

[5] Abd-Elaal, E., Mills, J.E., Ma, X., An analytical model for simulating steady state flows of downburst, *J. Wind Eng. Ind. Aerodyn.*, 115, 2013, 53–64.